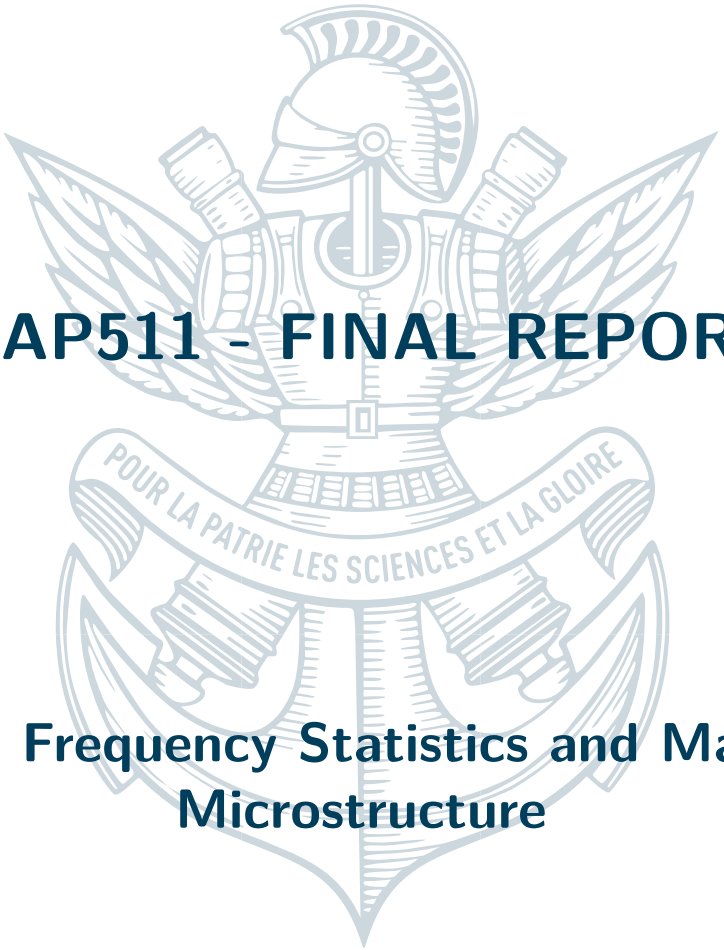


# MAP511 - FINAL REPORT

## High Frequency Statistics and Market Microstructure

17 December 2023

Under the supervision of Professor Mathieu ROSENBAUM
Nicolas MEIRA SINOTT LOPES | Ziad OUMZIL | Maxime MOUTET

# ACKNOWLEDGEMENTS

We would like to thank Professor Mathieu Rosenbaum for all the help, guidance, flexibility, and availability for our group during these past three months. We are very thankful for the opportunity to learn from him and we really appreciate all the guidance in the choice of the path of our study. The papers suggested were very interesting and sparked a true interest in academic research in the field, especially on the subject of volatility estimation under market microstructure influence. We believe it was a unique learning opportunity for us and we hope for the future X promotions that you will continue to supervise students in this course.

We would also like to thank Professor Aurélien Alfonsi for the paper suggestions that allowed us to properly simulate the discretization of asset price under the Heston model. We would also like to thank him for the course MAP552 - Stochastic Calculus in Finance which was crucial for the understanding of the papers and the research we conducted.

# EXECUTIVE SUMMARY

This report contains the research project of our group on the course MAP511 Initiation to Research - High Frequency Statistics and market microstructure, under the supervision of Professor Mathieu Rosenbaum.

We started our study by analyzing the paper "Optimal Execution of Portfolio Transactions" [1], understating how to model the risk aversion of a trader by the usage of a utility function. From that, we developed the equations to determine its optimal portfolio liquidation strategy under the permanent and temporary market impact of the trader's actions. We also obtained the expected loss as a function of a trader risk-averseness, what is called the *efficient frontier*. In the end, we observed the importance of a good volatility estimation given the sensibility of our utility function to its miscalculation, which led us to the study of volatility estimation for high-frequency trading scenarios.

We shifted therefore our focus towards the paper "A Tale of Two Time Scales" [2]. We reproduced some of the results of the paper, implementing the volatility estimators it proposes. Although under the theoretical assumptions of the paper the estimators worked quite well, we soon realized that market microstructure effects posed an important problem - the model did not account for the discretization of prices due to tick size. This led us to the study of two new papers: "A New Approach for the Dynamics of Ultra-High-Frequency Data: The Model with Uncertainty Zones" and "Volatility and covariation estimation when microstructure noise and trading times are endogenous" [3][4]. Thanks to the analysis of these two papers we were able to simulate asset price dynamics under the discretization of the tick size and learn a new estimator that took that into consideration. We present some plots that confirm the limits of our previous estimators and the robustness of the new one.

Finally, since some of our simulations required a discrete scheme of the Heston model, and simple Euler schemes of its volatility dynamics may lead to negative values, we shifted our study towards solving that problem. This was possible by using some of the schemes proposed by "On the discretization schemes for the CIR (and Bessel squared) processes", which we develop here some of the intuition and equations behind their construction [5]. In the end, we shifted our attention to the pricing of European call options of assets whose dynamics followed the Heston model. Since the characteristic function of the log price distribution of the asset can be determined analytically, we were able to perform that by using a Fast Fourier Transform technique, analyzing the papers "Option valuation using the fast Fourier transform", "Not-So-Complex Logarithms in the Heston Model", and "A closed-form solution for options with stochastic volatility with applications to bond and currency options" [6][7][8]. We provided the plots of the pricing using this method compared to a simple Monte Carlo, showcasing its advantages.

To access the full extent of our work, as well as the code that reproduces our simulations, please refer to our GitHub repository here.

# TABLE OF CONTENTS

# LIST OF FIGURES



# LIST OF TABLES

# 1 INTRODUCTION

## 1.1 Motivation

The aim of the course MAP511 - Initiation to Research is to provide an introduction to research and development in applied mathematics, through the completion of a project. The project consists of the study of a problem, motivated by applications or questions of a mathematical nature, ranging from modeling to implementation digital and critical analysis of the results.

The idea of using applied mathematics in finance sparked a true interest in the members of our group. All members took the course MAP552 - Stochastic Calculus in Finance during this period and were excited about applying many of the concepts to be acquired in the course in a research project. The subject of high-frequency trading, in particular, attracted us the most since it is of great importance in financial markets. For these reasons, we decided to apply for a project under the category "Financial Modeling and Engineering - High-Frequency Statistics and market microstructure".

## 1.2 Our study

During the past three months, we were invested in the understanding of several papers in the area of market microstructure. In this section, we will give a brief description of the timeline of our study. Each paper will be described in more detail in Section 2.

Initially, we delved into the study of the paper Optimal Execution of Portfolio Transactions [1]. We tried to understand how a trader would trade off expected cost and volatility under a particular utility function of their portfolio assuming temporary and permanent impact of their operations. We discovered when a trader is risk-averse, a new optimal solution, different than the one of minimal cost, is found. More interestingly, the solution is in particular very sensible to the estimation of the volatility, which we verified numerically and graphically. We became therefore interested in how to estimate the volatility of an asset within the context of high-frequency trading scenarios.

This led to the study of a second paper, a pioneer in the study of volatility estimation under the influence of market microstructure - Two Scales [2]. Here we understood and implemented five different estimators for the volatility and performed a Monte Carlo simulation under the Black-Scholes and Heston model to validate our results. Although interesting conceptually, we realized that such estimators assumed a theoretical description of asset pricing that did not resemble the true dynamics of prices under market microstructure influence. All estimators were modeled under a continuous price, whereas they should be discretized by the tick size under real market scenarios. Therefore, after the study of this paper, our group had two, somewhat

perpendicular, axes of study. The first is on how to properly simulate market microstructure behavior and estimate its intrinsic volatility, and the second is on the Heston model, given its simulation challenges.

On the first axe, we studied two papers: A New Approach for the Dynamics of Ultra-High-Frequency Data: The Model with Uncertainty Zones [3] and Volatility and covariation estimation when microstructure noise and trading times are endogenous [4]. These two papers allowed us to robustly simulate markets that are highly impacted by market microstructure and simulate appropriately the intrinsic volatility of the corresponding assets. We also compared these new estimators with the ones of our previous study, confirming the quality of the former, and the limitations of the latter.

Finally, the last part of our work was dedicated to the Heston model. Firstly, we studied how to appropriately discretize the price evolution of an asset under this model, something that was necessary for our previous studies. For that, we studied the paper On the discretization schemes for the CIR (and Bessel squared) processes [5]. Furthermore, we got interested in option pricing by using the Fast Fourier Transform, concluding our study with the analysis of the paper Option valuation using the fast Fourier transform [6]

## 1.3 Report Organization

We provide here the layout of our report to facilitate the reader when exploring different sections. This report is laid out in the chronological order of our study, hence we recommend the reader to follow as such. However, since most of the studies are somewhat independent, they can access each section in any order without much problem. This report is divided into three sections:

- Section 1: We developed the motivations of our group for following a project on MAP511 - Initiation to Research, as well as the timeline and brief explanation of our study.
- Section 2: A summary of all the papers we studied, highlighting their main idea. We also developed the studies and simulations that we performed.
- Section 3: A conclusion where we discuss the most interesting parts of our research, as well as some possible next steps.

# 2
# PAPERS STUDIED

## 2.1 Optimal Execution

In this section, we develop our study of the paper Optimal Execution. We will follow the same notation as in the paper. A more detailed proof of the equations we present here can be found either in our GitHub repository here or in the paper. As briefly discussed in Section 1.2, in this section we study the trade-off between the expected cost and volatility of a trader when trying to liquidate a portfolio with the help of a utility function that encapsulates the risk-aversion of the trader. We will develop on the model that was used to simulate the market impact of the trader (2.1.1), how a trader will liquidate its position depending on their risk aversion under the optimal execution (2.1.2), what is their expected trading cost as a function of their risk aversion (2.1.3), and how would their utility function be impacted if they miscalculated the asset's volatility (2.1.4).

### 2.1.1 • Description of the model

In the paper, the liquidation of a portfolio is modeled by a discretization into $N$ steps. The sequence $(x_k)_{k\in\{1,\dots,N\}}$ represents the number of shares we still hold at each step, hence $x_0 = X$, where $X$ is the total amount of shares we hold, and $x_N = 0$. We also define $n_k = x_{k-1} - x_k$ to be the amount of shares we trade at a given step $k$. The price evolution of the asset in this discretized configuration has the dynamics of a discrete arithmetic random walk:

$$S_k = S_{k-1} + \sigma\tau^{\frac{1}{2}}\xi_k - \tau g\left(\frac{n_k}{\tau}\right)$$

We take $\sigma$ to be the volatility of the asset, $\tau = \frac{N}{T}$ each time step, $(\xi_i)_{i\in\{1,\dots,N\}}$ a sequence of i.i.d random variables of mean zero and unit variance[1]. The term $g$ contains the **permanent impact** of our strategy on the price of the asset.

As in the paper, we take a linear function for $g$, $g(v) = \gamma v$, hence:

$$S_k = S_0 + \sigma\sum_{j=1}^{k}\tau^{\frac{1}{2}}\xi_j - \gamma(X - x_k)$$

Where $X$ is the initial portfolio size and $x_k$ is the amount of units of the asset we still hold.

Furthermore, we also take into account a **temporary impact** of our transactions, which we take to be linear:

$$\tilde{S}_k = S_{k-1} - h\left(\frac{n_k}{\tau}\right) = S_{k-1} - \epsilon\mathrm{sgn}(n_k) - \frac{\eta}{\tau}n_k$$

[1]For our simulations we will stick to the standard normal distribution

We assume therefore that the price that we actually capture at step $k$ is $\tilde{S}_k$.

Under these assumptions, the cost of trading, which is the difference between the full book value and the *capture* of our trajectory, becomes therefore:

$$C = XS_0 - \sum_{k=1}^{N} n_k \tilde{S}_k = -\sum_{k=1}^{N} \left(\sigma \tau^{\frac{1}{2}} \xi_k - \tau g\left(\frac{n_k}{\tau}\right)\right) x_k + \sum_{k=1}^{N} n_k h\left(\frac{n_k}{\tau}\right)$$

Its expected value and variance are:

$$\mathbb{E}[C] = \sum_{k=1}^{N} \tau g\left(\frac{n_k}{\tau}\right) x_k + \sum_{k=1}^{N} n_k h\left(\frac{n_k}{\tau}\right)$$

$$\mathbb{V}[C] = \tau \sigma^2 \sum_{k=1}^{N} x_k^2$$

In the linear case:

$$\mathbb{E}[C] = \frac{1}{2}\gamma X^2 + \epsilon X - \left(\frac{\eta}{\tau} - \frac{1}{2}\gamma\right) \sum_{k=1}^{N} n_k^2$$

Please refer to our GitHub repository here if you wish for a full proof of these results.

### 2.1.2 • Optimal portfolio evolution

One may directly affirm that the optimal strategy would be to minimize the expectation of shortfall, but in this case, this strategy will lead to a high variance and, hence a high risk. On the other hand, minimizing variance will lead to maximizing the expectation of shortfall. Hence, an optimal strategy does not have a meaning without introducing $\lambda$ that would encapsulate the *risk aversion* of the trader. We introduce an utility function $U := \mathbb{E}[x] + \lambda \mathbb{V}[x]$ and the optimal strategy is the solution of:

$$\min_x \left(\mathbb{E}[x] + \lambda \mathbb{V}[x]\right)$$

Where $x$ represents a possible trajectory for the portfolio liquidation. If $\lambda > 0$ the objective function is strictly convex, hence there is a unique optimal solution $x^*(\lambda)$.

Let us assume that we hold a positive value of the actions of the given asset in our book, and our goal is to liquidate it. We will assume from now on that at each step $k$ the sign of $n_k$ is the same, and the permanent and temporary impacts are linear as described previously. We determine the unique global minimum by setting the partial derivatives of the objective function to zero, and after solving some system of equations, we get :

$$x_j = \frac{\sinh(\kappa(T - t_j))}{\sinh(\kappa T)} X; \quad j = 0, \ldots, N$$

Hence

$$n_j = \frac{2\sinh(\frac{1}{2}\kappa\tau)}{\sinh(\kappa T)}\cosh(\kappa(T - t_{j-\frac{1}{2}}))X$$

Where $t_{j-\frac{1}{2}} = (j - \frac{1}{2})\tau$ and where $\kappa$ is defined by this system

$$\begin{cases} \frac{2}{\tau^2}\left(\cosh(\kappa\tau) - 1\right) = \tilde{\kappa}^2 \\ \tilde{\kappa}^2 = \frac{\lambda\sigma^2}{\tilde{\eta}} = \frac{\lambda\sigma^2}{\eta(1-\frac{\gamma\tau}{2\eta})} \end{cases}$$

The corresponding expectation and variance :

$$E(X) = \frac{1}{2}\gamma X^2 + \epsilon X + \tilde{\eta}X^2\frac{\tanh(\frac{1}{2}\kappa\tau)\left(\tau\sinh(2\kappa T) + 2T\sinh(\kappa\tau)\right)}{2\tau^2\sinh^2(\kappa\tau)}$$

$$V(X) = \frac{1}{2}\sigma^2X^2\frac{\tau\sinh(\kappa T)\cosh(\kappa(T-\tau)) - T\sinh(\kappa\tau)}{\sinh^2(\kappa T)\sinh(\kappa\tau)}$$

Please refer to our GitHub repository here if you wish for a full proof of these results. In Figure 1 we have the curve that we obtained for the lowest possible cost (no risk aversion) and a risk aversion proposed by the paper following the same parameters as in the paper.

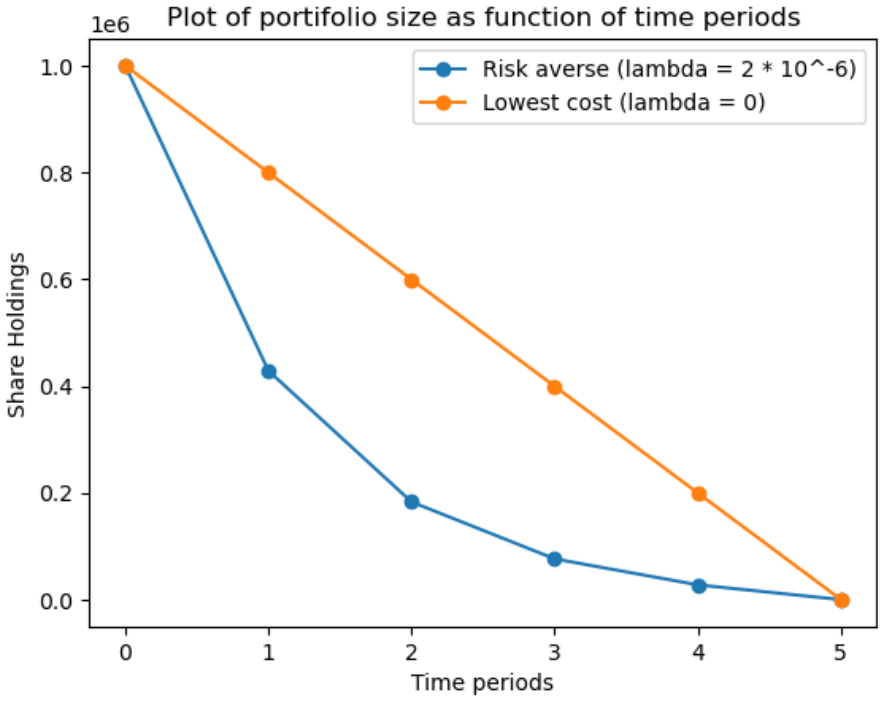


Figure 1: Portfolio size evolution for different risk aversion parameters.

### 2.1.3 • The efficient frontier

Next, we attempt to reproduce the *Efficient Frontier*, which corresponds to the plot of the expected loss of a trader as a function of the variance that they are willing to hold under the optimal portfolio execution. The plot we obtained in Figure 2 is the same as obtained in the paper.

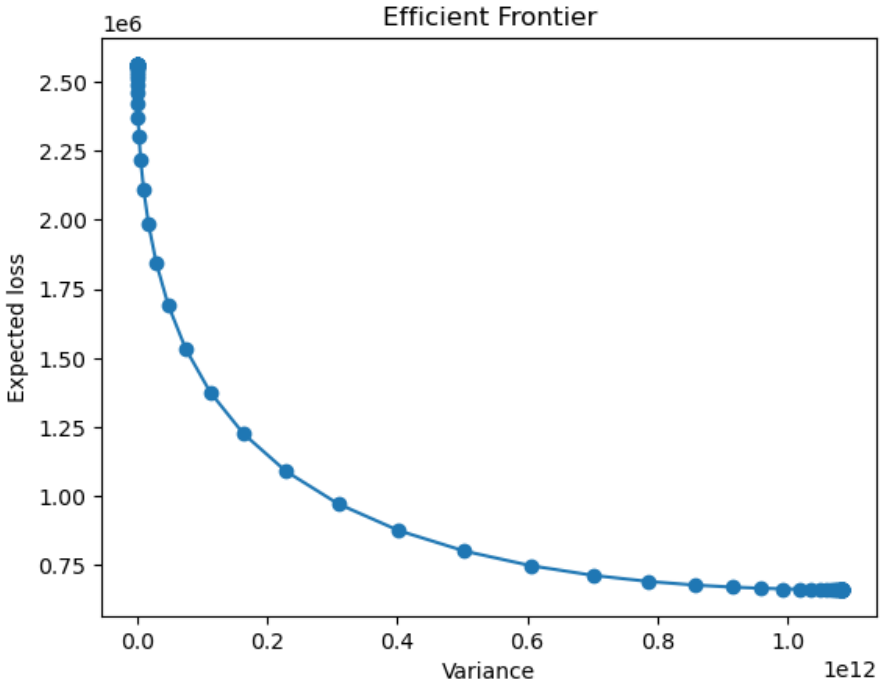


Figure 2: Efficient frontier plot.

### 2.1.4 • Impact of volatility miscalculation

The efficient frontier plot assumes that a trader is fully capable of estimating the intrinsic variance of the asset it is trading. What would happen if the trader miscalculated the volatility and proceeded to trade under the assumption it was correct, how would its utility function be sensible to that mistake? This question is answered by the plot obtained in Figure 3.

We conclude from the plot that the utility function is very dependent on the asset volatility we calculate.

### 2.1.5 • Conclusion

In the study of this paper, we arrived at two very interesting conclusions. The first is that assuming that a trader can correctly estimate the asset's volatility and other market parameters, they can obtain an optimal portfolio liquidation execution for a given variance tolerance (risk averse). The second conclusion is that, unfortunately, their utility function is very sensitive to

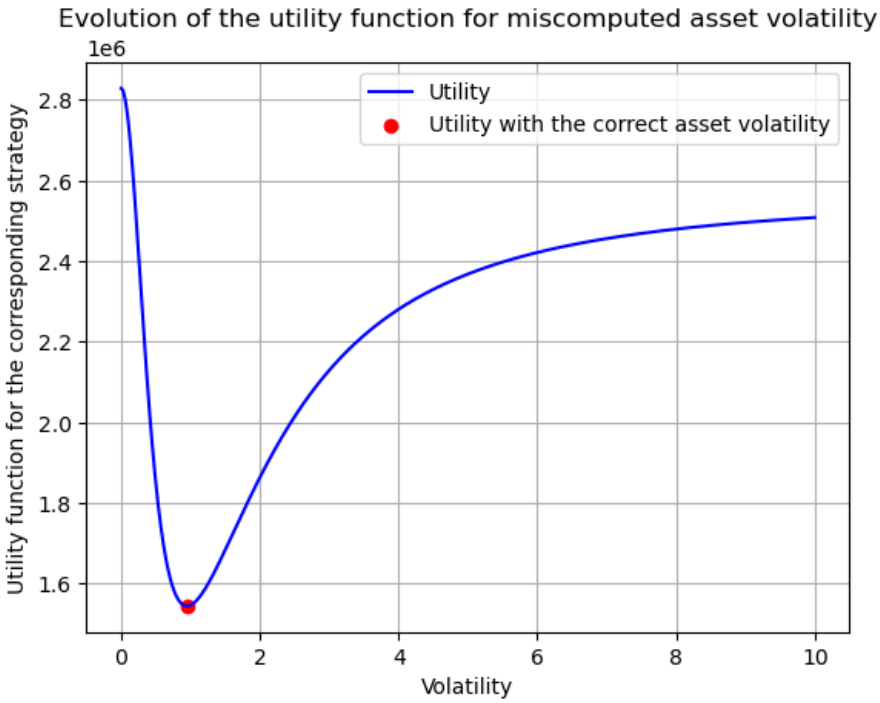


Figure 3: Impact of volatility miscalculation on the utility function.

the miscalculation of the asset's volatility. This made us aware of the importance of a precise volatility estimation in trading a certain asset, which led us to the study of the next paper, described in Section 2.2. [1]

## 2.2 Integrated Volatility

In this section, we develop our study of the paper A Tale of Two Time Scales: Determining Integrated Volatility With Noisy High-Frequency Data [2]. Detailed Simulation can be found in our GitHub repository here.

As we have resumed in the introduction, this paper is considered a pioneer in the study of volatility estimation under the influence of market microstructure. The paper makes the following assumption, that **the observed return** $Y_t$ is equal to $X_t + \epsilon_t$, where $X_t$ is **the true value of the return** and $\epsilon_t$ incorporates the **"observation error"** due to market microstructure.

$$Y_t = X_t + \epsilon_t$$

Hence to accurately estimate the integrated volatility, we have to take into consideration this observation error.

### 2.2.1 • Definition of Integrated Volatility

If $S_t$ is the asset price, we suppose that the return $X_t = log(S_t)$ follows an Ito process :

$$dX_t = \mu_t dt + \sigma_t dW_t$$

Then the integrated volatility over a time interval from 0 to T, is defined by :

$$IV = \int_0^T \sigma_t^2 dt$$

The estimator of this object is the quadratic variation defined by :

$$[X, X]_T = \sum_{t_i} (X_{t_{i+1}} - X_{t_i})^2$$

Where $0 \leq t_0 < ... < t_n \leq T$ are times of observations.

The problem is that we don't have access to $X_{t_i}$, we only observe $Y_{t_i}$, which is equal to $X_{t_i} + \epsilon_{t_i}$, we make the assumption that $\epsilon_{t_i}$'s are iid noise with $E\epsilon_{t_i} = 0$, and $var(\epsilon_{t_i}) = E\epsilon^2$ $(*)$, and independent from the true returns $X$. The purpose of this paper is to propose, under these assumptions, five estimators, ranked from the worst to the best.

### 2.2.2 • Fifth best estimator $[Y, Y]_T^{(all)}$ : Completely Ignoring the Noise.

This naive estimator of quadratic variation is $[Y, Y]_T^{(all)}$, which is the realized volatility based on the entire sample

$$[Y, Y]_T^{(all)} = \sum_{i=0}^{n-1} (Y_{t_{i+1}} - Y_{t_i})^2 \qquad (1)$$

To prove that this estimator is very bad, we will show that

$$[Y,Y]_T^{(all)} = \sum_{i=0}^{n-1}(Y_{t_{i+1}} - Y_{t_i})^2 = 2nE\epsilon^2 + O_p(n^{1/2})$$

*Proof. (from the paper)* Under the additive model $Y_{t_i} = X_{t_i} + \epsilon_{t_i}$ the realized volatility based on the observed returns now has the form :

$$[Y,Y]_T^{(all)} = [X,X]_T^{(all)} + 2[X,\epsilon]_T^{(all)} + [\epsilon,\epsilon]_T^{(all)}$$

Subject to the assumptions $(*)$, and $E\epsilon^4 < \infty$ :

$$E([Y,Y]_T^{(all)}|X \text{ process}) = [X,X]_T^{(all)} + 2nE\epsilon^2$$

$$Var([Y,Y]_T^{(all)}|X \text{ process}) = 4nE\epsilon^4 + O_p(1)$$

Therefore as $n \to \infty$, conditionally on the $X$ process, we have the following asymptotic normality in law :

$$n^{-1/2}\left([Y,Y]_T^{(all)} - 2nE\epsilon^2\right) \to 2(E\epsilon^4)^{1/2}Z_{noise}$$

Where $Z_{noise}$ follows a normal distribution. □

(1) shows, theoretically, that this estimator estimates the noise and completely ignores the IV. Along with this theoretical observation, we will demonstrate it with a simulation.

### 2.2.3 • Fourth Best Estimator $[Y,Y]_T^{(\text{sparse})}$ : Sampling Sparsely at Some Lower Frequency.

Constructing lower-frequency returns from the available data. Taking only several observations, for example, an observation every 5 minutes, and computing the quadratic variation.

$$0 \le t_{i_1} < ... < t_{i_{n_{sparse}}} = T$$

$$[Y,Y]_T^{(sparse)} = \sum_{j=1}^{n_{sparse}-1}(Y_{t_{i_j}} - Y_{t_{i_{j+1}}})^2$$

### 2.2.4 • Third Best Estimator $[Y,Y]_T^{(sparse,opt)}$ : Sampling Sparsely at an Optimally Determined Frequency.

It is feasible to identify an ideal sampling frequency instead of choosing the frequency somewhat arbitrarily, as done in the fourth-best approach. In effect, this is similar to the fourth-best approach, except that the arbitrary $n_{sparse}$ is replaced by an optimally determined $n^*_{sparse}$. This optimal sampling frequency is calculated to minimize the MSE, and is given by the following formula :

$$n^*_{sparse} = \left(\frac{T}{4E\epsilon^2}\int_0^T \sigma_t^4 dt\right)$$

**Remark.** *The computation of $n^*_{sparse}$ needs the estimation of $E\epsilon^2$, but also, it needs the estimation of the integrated quarticity $\int_0^T \sigma_t^4 dt$. The first parameter, can be estimated using $[Y,Y]_T^{(all)}/(2n)$. For the IQ estimations we used in our simulation the quartic variation, and also a more complex estimation method proposed in the paper, and compared it when we used the real value of the IQ.*

### 2.2.5 • Second Best Estimator $[Y,Y]_T^{(avg)}$ : Subsampling and Averaging.

The third estimator constructed by averaging the estimators $[Y,Y]_T^{(k)}$ across K grids of average size $\bar{n}$.

$$[Y,Y]_T^{(avg)} = \frac{1}{K}\sum_{k=1}^{K}[Y,Y]_T^{(k)}$$

Where

$$[Y,Y]_T^{(k)} = \sum_{i=0}^{n/K}(Y_{t_{k+i(K+1)}} - Y_{t_{k+iK}})^2$$

The optimal choice of K is as follow : $K^* = n/\left(\frac{T}{6*(E\epsilon^2)^2}\int_0^T \sigma_t^4 dt\right)$

### 2.2.6 • First Best Estimator $\widehat{\langle X,X\rangle}^{(adj)}$ : Subsampling and Averaging, and Bias-Correction.

The paper proposes a final estimator based on a bias correction,

$$\widehat{\langle X,X\rangle} = \left([Y,Y]_T^{(avg)} - \frac{\bar{n}}{n}[Y,Y]_T^{(all)}\right)$$

This estimator is then adjusted, to get the first best estimator

$$\widehat{\langle X,X\rangle}^{(adj)} = (1-\frac{\bar{n}}{n})\left([Y,Y]_T^{(avg)} - \frac{\bar{n}}{n}[Y,Y]_T^{(all)}\right)$$

The paper shows that as $n \to \infty$

$$\widehat{\langle X,X\rangle}_T = \langle X,X\rangle + \frac{1}{n^{1/6}}\left(\frac{8}{c^2}(E\epsilon 2)^2 + c\frac{4T}{3}\int_0^T \sigma_t^4 dt\right)^{1/2} Z_{total}$$

### 2.2.7 • Parameters estimation

The first, second, and third-best estimators optimally chose their parameters, which all need the estimation of $IQ = \int_0^T \sigma_t^4 dt$
In our simulation, we used the real value of the IQ and compared the performance when using these two following estimators of IQ.

As well as the paper's estimator of the IQ. Estimating integrated quarticity (IQ) $\int_0^T \sigma_t^4 dt$ - This estimator is proposed on section 6 of the paper

$$IQ = \widehat{\int_0^T \sigma_t^4 dt} = \frac{\hat{s}_0^2 - 8E(\epsilon^2)^2 c_1^{-2}(1 + I^{-2} - I^{-1})}{c_1(I^{1/2} - 1)T}$$

where

$$\hat{s}_0^2 = n^{1/3} \sum_{m=1}^{M-1} \left( (\langle X, X \rangle_{T_{m+1}}^{K_1} - \langle X, X \rangle_{T_m}^{K_1}) - (\langle X, X \rangle_{T_{m+1}}^{K_2} - \langle X, X \rangle_{T_m}^{K_2}) \right)^2$$

Estimating integrated quarticity (IQ) $\int_0^T \sigma_t^4 dt$ using a low frequency

$$IQ = \frac{n_{sparse}}{3} \sum_{j=0}^{n_{sparse}-1} (Y_{t_{i_j}} - Y_{t_{i_{j+1}}})^4$$

### 2.2.8 • Comparison and Conclusion

The simulation uses an asset price that follows a Black&Scholes process

$$dS_t = \mu S_t dt + \sigma S_t dW_t$$

and hence $X_t$ follows

$$dX_t = \left( \mu - \frac{1}{2}\sigma^2 \right) dt + \sigma dW_t$$

with $\mu = 0.05$ and $\sigma = 0.04$.

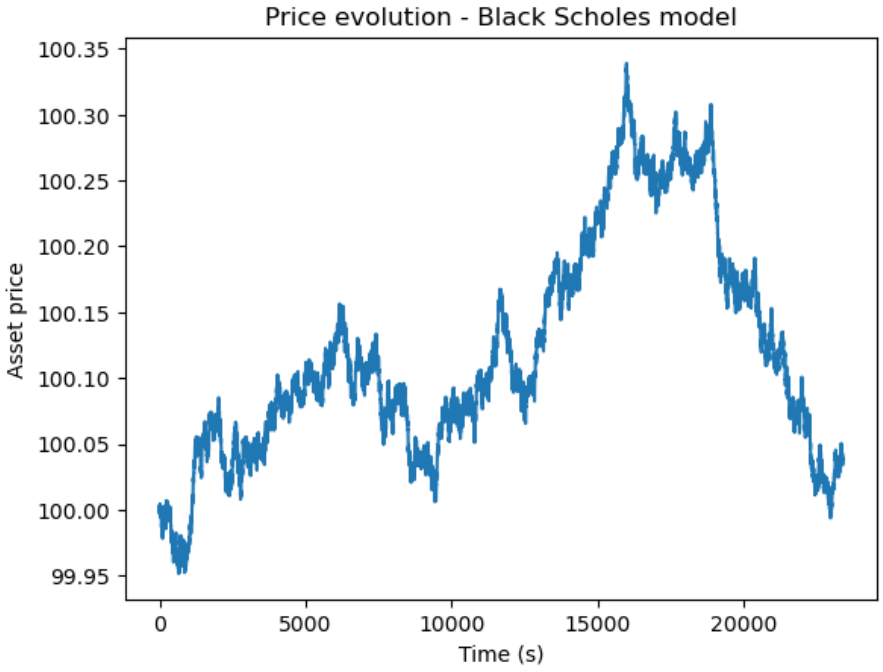

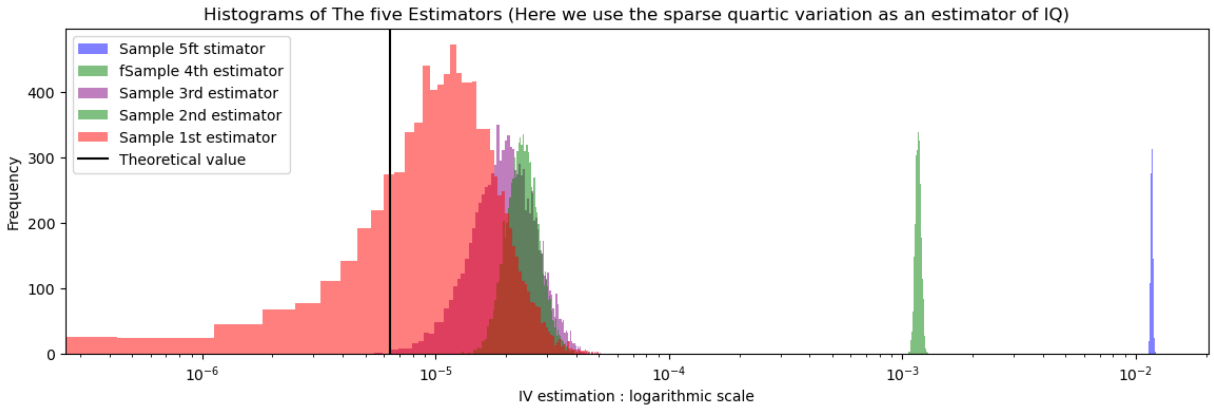


Figure 4: The five estimators performance, here we use the sparse quadratic variation to estimate IQ. The x-axis is in a logarithmic scale.

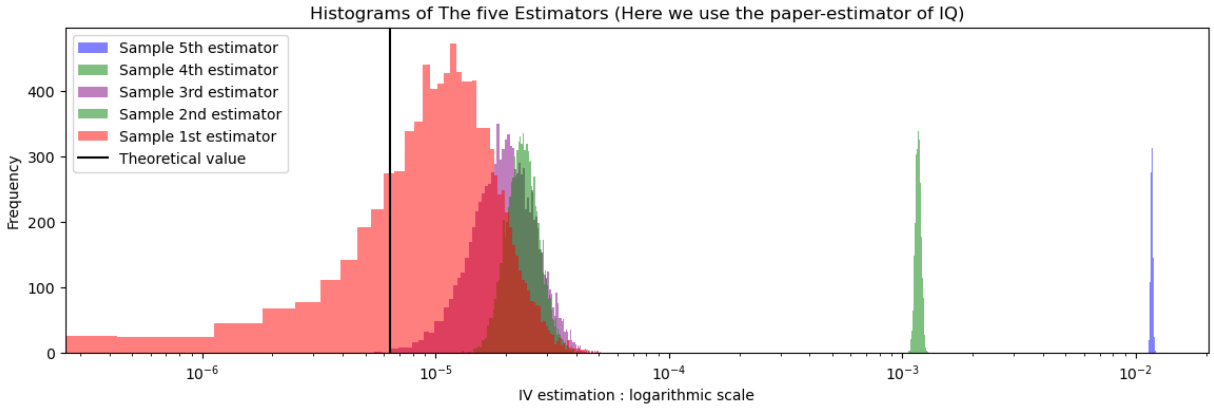


Figure 5: The five estimators performance, here we use the paper's estimator of the IQ. The x-axis is in a logarithmic scale.

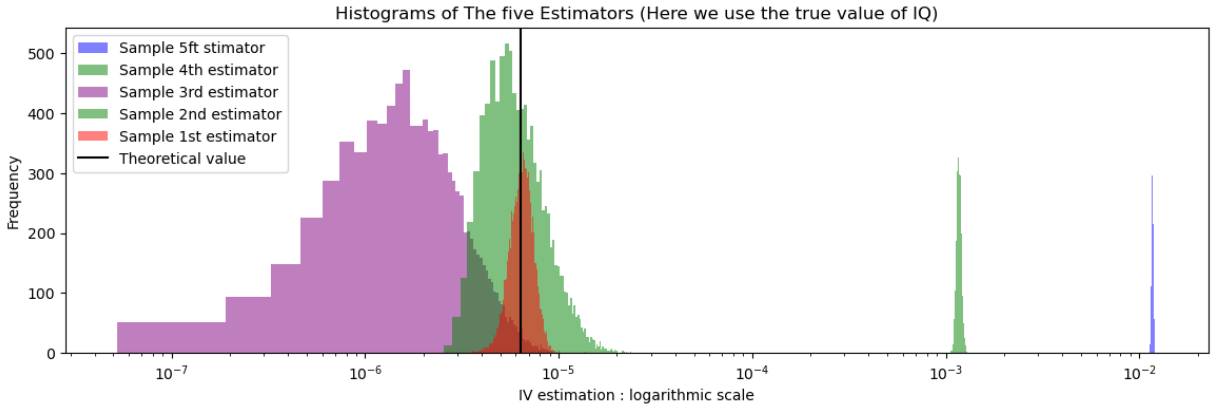


Figure 6: The five estimators performance, here we use the real value of the IQ. The x-axis is in a logarithmic scale.

**Remark.** *"As we have theoretically demonstrated, neither the fifth nor the fourth estimators can be used to estimate the integrated volatility. By selecting an optimal sparsity, the third estimator becomes acceptable. The second and first estimators are very effective, and their accuracy is further enhanced when using the true value of the integrated quarticty, IQ*

### 2.2.9 • Simulation with a Heston Model

The paper "Two Scales" [2] utilizes the Heston stochastic volatility model, as the data-generating process. Simulating the Heston model presented a significant challenge due to numerical errors encountered when applying the basic Euler discretization method to solve the associated stochastic differential equations (SDEs).

We subsequently focused our study on the Heston Model, exploring various simulation methods and option pricing techniques.

Afterward, we employed the five integrated volatility estimators to produce the comparison table below.

Table 1: Comparison of The Integrated Volatility Estimators

| Metric | Fifth-best | Fourth-best | Third-best | Second-best | First-best |
|---|---|---|---|---|---|
| Bias | 0.011 704 | 0.001 027 | −0.000 136 | 0.000 011 | −0.000 003 |
| Std | 0.000 136 | 0.000 037 | 0.000 014 | 0.000 032 | 0.000 009 |
| RMSE | 0.011 704 | 0.001 028 | 0.000 137 | 0.000 034 | 0.000 001 |
| Relative bias | 74.405 751 | 6.536 791 | −0.860 181 | 0.071 141 | −0.021 883 |
| Relative variance | 47.315 819 | 0.520 994 | 0.001 532 | 0.041 699 | 0.003 342 |
| Relative RMSE | 74.723 032 | 6.576 521 | 0.861 071 | 0.216 242 | 0.061 812 |

### 2.2.10 • Limitations

As discussed in our introductory section, this paper attempts to address the influence of market microstructure. However, in the next session, we will explore Professor Mathieu Rosenbaum's paper, which introduces a new model that more accurately describes the observed returns in high-frequency data.

## 2.3 Uncertainty Zones

Given the limitations we encountered in the model described in the previous section (Section 2.2.10), we shifted our studies to two new papers - A New Approach for the Dynamics of Ultra-High-Frequency Data: The Model with Uncertainty Zones [3] and Volatility and covariation estimation when microstructure noise and trading times are endogenous [4]. The model used in both papers allowed us to simulate the dynamics of the high-frequency trading markets that are impacted by market microstructure factors (2.3.1). Moreover, we were able to estimate the main parameters that influence the behavior of such markets 2.3.3, as well as compare the quality of the estimators proposed in the previous section (2.2) to the new one proposed (2.3.4).

The main conclusions and findings of this section were that now we were capable of better simulate markets that are subjected to the discretization of asset price by the tick size, an important factor of market microstructure. Moreover, we were also able to verify that the new volatility estimator proposed worked much better than the ones proposed in the previous section (2.2). The first best estimator (2.2.6) still gave, despite its modeling limitations, a fair estimate of the volatility.

### 2.3.1 • The model

In this section, we will give a brief description of the model described by the papers following the same notation. Please refer to A New Approach for the Dynamics of Ultra-High-Frequency Data: The Model with Uncertainty Zones [3] for a more detailed and in-depth description.

Let $(X_t)_{t\geq 0}$ be the efficient price of the asset. Let $(\Omega, (\mathcal{F}_t)_{t\geq 0}, \mathbb{P})$ be the filtered probability space, and $(W_t)_{t\geq 0}$ a standard $\mathcal{F}$-Brownian motion. We assume that the logarithm of the price is $\mathcal{F}_t$-adapted continuous semi-martingale that follows the equation:

$$Y_t = \log(X_t) = \log(X_0) + \int_0^t a_u dt + \int_0^t \sigma_{u-} dW_u$$

We define the tick grid as $\{k\alpha, k \in \mathbb{N}\}$ with $\alpha$ the tick size. We now define the uncertainty zones in between the mid-points of the tick grid as $\mathcal{U}_k = [0, +\infty) \times (d_k, u_k)$ with:

$$d_k = \left(k + \frac{1}{2} - \eta\right)\alpha \quad \text{and} \quad u_k = \left(k + \frac{1}{2} + \eta\right)\alpha, \quad \text{with} \quad 0 < \eta < 1$$

Let us now define the sequence of exit times from uncertainty zones $(\tau_i)_{i\geq 0}$. We take $\tau_0 = 0$ and we assume that we start at the tick $k_0 = X_0^{(\alpha)}/\alpha$, $X_0^{(\alpha)}$ being $X_0$ rounded to the nearest multiple of $\alpha$. Let $\tau_1$ be the first exit time from the set $(d_{k_0-1}, u_{k_0})$.

We then define recursively $\tau_{i+1}$ as the exit time of $(X_t)_{t>\tau_i}$ of the uncertainty zone $(d_{k_i-L_i}, u_{k_i+L_i-1})$, where $k_i = X_{\tau_i}^{(\alpha)}/\alpha$ and $L_i$ representing the absolute value in number of ticks of the price jump between the $i^{th}$ and the $(i+1)^{th}$ transaction leading to a price change.

$$\tau_{i+1} = \inf\left\{t : t > \tau_i, \quad X_t = \left(k_i - L_i - \frac{1}{2} + \eta\right)\alpha \quad \text{or} \quad X_t = \left(k_i + L_i - \frac{1}{2} + \eta\right)\alpha\right\}$$

For the simulations we conducted, we will assume that the price can only jump from one tick to one consecutive tick ($L_i = 1$). We also assume that the transactions that lead to a change of price are exactly made at the times $\tau_i$. We call by $(P_{\tau_i})_{i\in\mathbb{N}}$ the prices of these transactions.

From this, we can retrieve the efficient price at times $\tau_i$:

$$X_{\tau_i} = P_{\tau_i} - \text{sign}(P_{\tau_i} - P_{\tau_{i-1}}) \left(\frac{1}{2} - \eta\right) \alpha$$

### 2.3.2 • Simulations

In this section, we attempt to reproduce the curves that were presented in the paper [3]. We will assume an asset whose true price evolves as:

$$dX_t = \sigma_t X_t dW_t, \quad X_0 = 100, \quad t \in [0, 1]$$

Where $(\sigma_t)_{t\in[0,1]}$ is a deterministic function. The interval $[0, 1]$ corresponds to one trading day of 8h. Here we study two functions $\sigma_t$. One that reproduces attempts to reproduce the results of the paper, which are shown in this section, and another of constant value to compare different volatility estimators that are used in the following sections.

Figure 7 shows the plot of the volatility that we chose, as well as the plot of the duration for a trade to occur as a function of time. They reproduce fairly well the curves obtained in the paper.

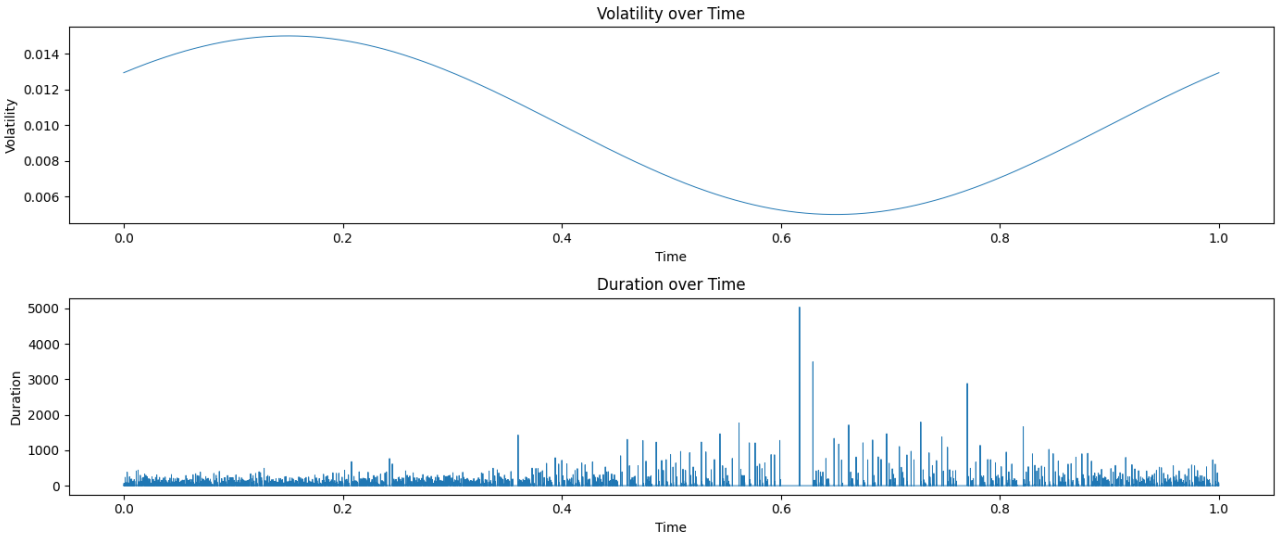


Figure 7: Volatility of the asset and time to price change.

Furthermore, Figure 8 allows us to visualize the price of the asset under the effects of the discretization of the price by the tick size as modeled by the uncertainty zones.

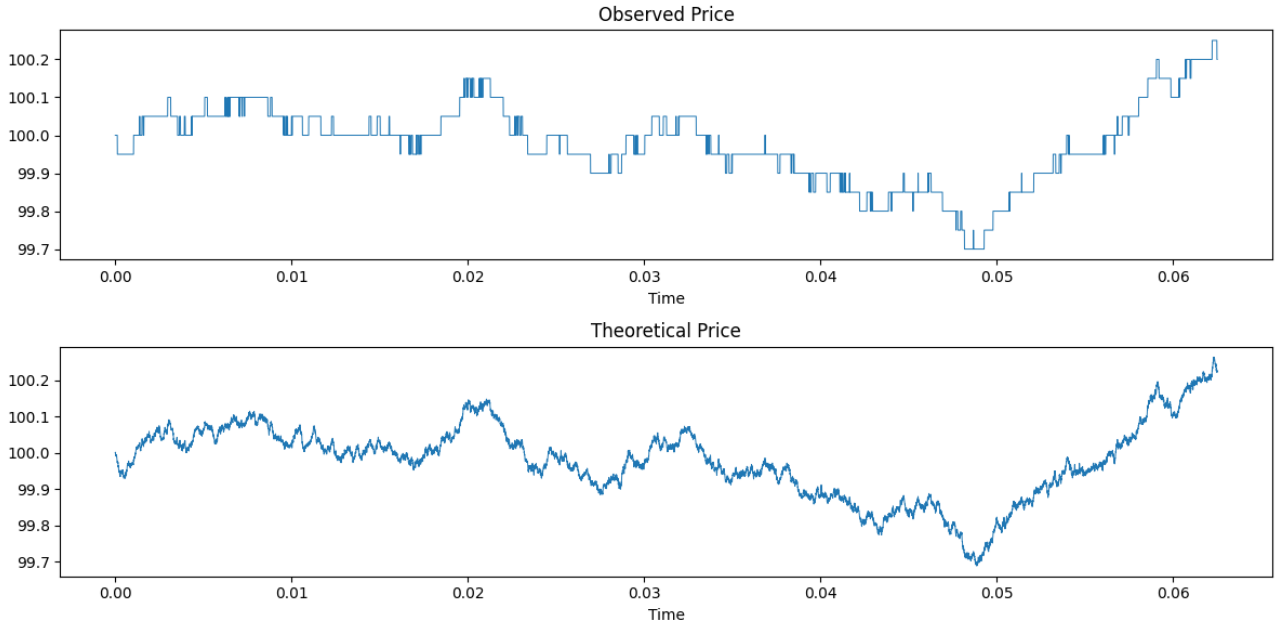


Figure 8: Observed price versus the theoretical price of the asset.

### 2.3.3 • Estimating parameters and asset volatility

In the following sections, we take the asset's daily volatility to be constant and equal to 3%. Hence, the theoretically integrated volatility corresponds to $9 \times 10^{-4}$.

**Estimating $\eta$:** To estimate $\eta$, we assume that the jump sizes of two consecutive price is bounded, and we denote $m$ as the maximum jump. In practice, with a small volatility, jumps that exceed two are very rare. Here we take the estimators as proposed in the paper [4].

We define $N^{(a)}_{\alpha,t,k}$ and $N^{(c)}_{\alpha,t,k}$ :

$$N^{(a)}_{\alpha,t,k} = \sum_{t_i \leq t} \mathbb{I}_{\{(P_{t_i} - P_{t_{i-1}})(P_{t_{i-1}} - P_{t_{i-2}}) < 0 \text{ and } |P_{t_i} - P_{t_{i-1}}| = k\alpha\}}$$

$$N^{(c)}_{\alpha,t,k} = \sum_{t_i \leq t} \mathbb{I}_{\{(P_{t_i} - P_{t_{i-1}})(P_{t_{i-1}} - P_{t_{i-2}}) > 0 \text{ and } |P_{t_i} - P_{t_{i-1}}| = k\alpha\}}$$

For $k = 1, \ldots, m$.

We define the estimator of $\eta$ by :

$$\hat{\eta}_{\alpha,t} = \min\left(\max\left(0, \sum_{k=1}^{m} \lambda_{\alpha,t,k} u_{\alpha,t,k}\right), 1\right)$$

Where

$$\lambda_{\alpha,t,k} = \frac{N^{(a)}_{\alpha,t,k} + N^{(c)}_{\alpha,t,k}}{\sum_{j=1}^{m}(N^{(a)}_{\alpha,t,j} + N^{(c)}_{\alpha,t,j})} \text{ and } u_{\alpha,t,k} = \frac{1}{2}\left(k\left(\frac{N^{(c)}_{\alpha,t,k}}{N^{(a)}_{\alpha,t,k}} - 1\right) + 1\right)$$

**Estimating asset volatility** In this section, we will analyze the curves obtained by two different estimators for the volatility using the estimated $\eta$ as proposed by the paper[3]. As indicated, a simple way to estimate the volatility is by taking the realized volatility measure over the estimated values of the efficient price $X_{\tau_i} = P_{\tau_i} - \text{sign}(P_{\tau_i} - P_{\tau_{i-1}}) \left(\frac{1}{2} - \eta\right) \alpha$:

$$\sum_{\tau_i \leq t} \left( \frac{\hat{X}_{\tau_i} - \hat{X}_{\tau_{i-1}}}{\hat{X}_{\tau_{i-1}}} \right)^2$$

Figure 9 shows a Monte Carlo simulation that displays the estimation of the volatility. We can clearly see that the volatility estimation proposed fits very well the theoretical value.

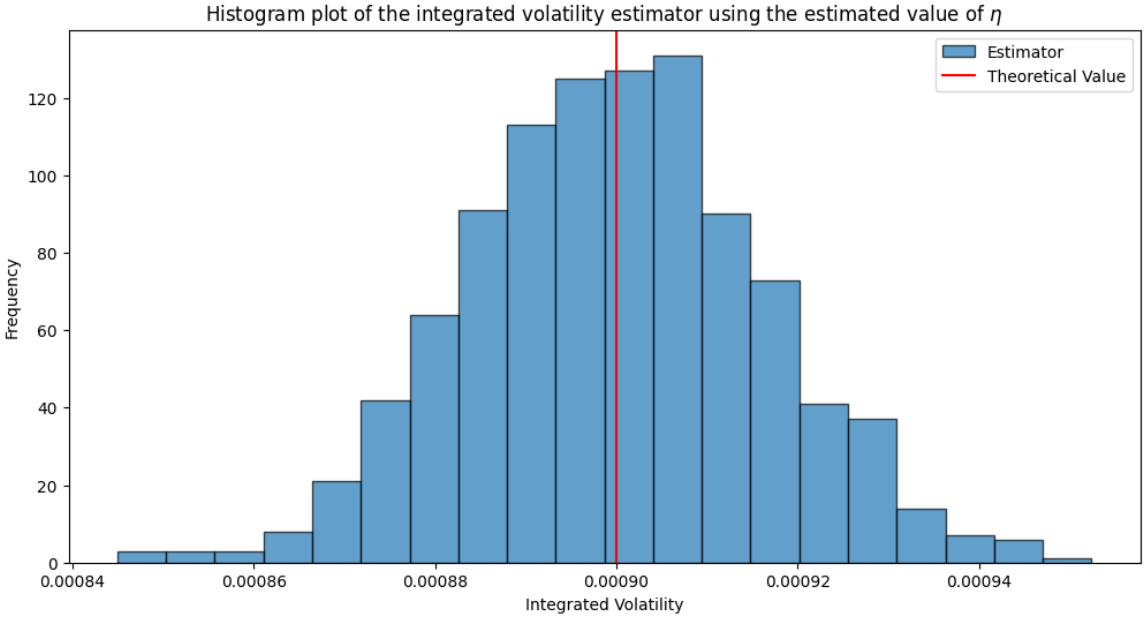


Figure 9: Estimation of asset volatility for new estimator - 1000 simulations.

### 2.3.4 • Comparing volatility estimators

Finally, we would like to compare the volatility estimators that we obtained in Section 2.2 with the one in this section. The idea is to see how the estimators would be impacted by the effect of price discretization under the uncertainty zones model. Figure 10 shows the difference between the three best estimators from the previous method against the one proposed in this section.

From the plot we obtained, the best estimator is the one proposed in this section. Moreover, although the second-best estimator of the previous section still manages to give a fair estimate of the volatility, it is clear that they fail in general to predict the integrated volatility. This was rather expected since in the model used to derive such estimators assumed a price that was not discretized. Since prices of real markets are discretized by the tick size, the estimator

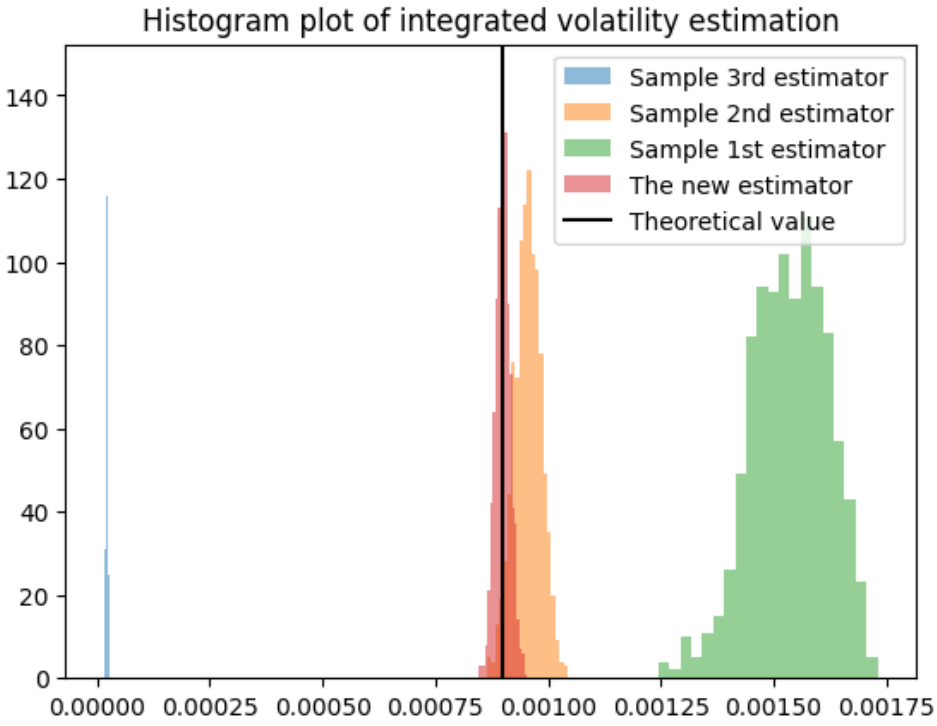


Figure 10: Monte Carlo simulation plot of volatility estimators - 1000 simulations.

proposed in this section seems more appropriate if one desires to estimate the volatility of an asset under high-frequency trading.

It might come as a surprise that the second estimator performs better than the first. It is, however, rather expected since the first estimator optimizes its parameters assuming a model that does not correspond to the true price evolution of an asset under market microstructure influence.

## 2.4 CIR Scheme for Heston Model

The Heston model, introduced by Steven Heston in 1993, is a mathematical model used in quantitative finance to describe the dynamics of financial markets, particularly the pricing of options. Unlike the simpler Black-Scholes model, the Heston model incorporates stochastic volatility, meaning that it allows for the volatility of the underlying asset to vary randomly over time. This dynamic feature addresses one of the limitations of the Black-Scholes model, which assumes constant volatility. Let $T > 0$ finite, $S_t, t \in [0, T]$ the price, and $\nu_t, t \in [0, T]$ the variance of an asset following the Heston model. Its dynamics are as follows:

$$dS_t = \mu S_t dt + \sqrt{\nu_t} S_t dW_t^S$$

$$d\nu_t = \kappa(\theta - \nu_t)dt + \epsilon\sqrt{\nu_t} dW_t^\nu$$

Where $W_t^S$ is the Brownian motion associated with the dynamics of the price and $W_t^\nu$ with the dynamics of the variance. Furthermore:

- $\theta$: is the variance to which $\nu_t$ reverse to.
- $\kappa$: the rate of that reversion.
- $\rho$: the correlation between the two Brownian motions.
- $\epsilon$: the volatility of the volatility, which is assumed to be constant.

Most of the results we presented in Sections 2.2 and 2.3 used the Black-Scholes model for the evolution of the asset price. In the paper "A Tale of Two Time Scales" [2], however, the price of the asset followed the Heston model. As we wanted to reproduce some of the results obtained in this paper, we got interested in learning how to find a scheme to simulate it. At first, we thought about simply implementing an Euler scheme, similar to what is usually done with a Black-Scholes model. Soon we realized the limitations of such an approach: the volatility can assume negative values under such discretization. [5]

Aware of this limitation, we engaged in researching how to solve this problem. The main focus of our study was on simulating the volatility, which follows a Cox-Ingersoll-Ross process, through the paper "On the discretization schemes for the CIR (and Bessel squared) processes" [5], the topic of this section. Armed with the tools acquired here, we were able to simulate the Heston model and reproduce some of the results that we obtained in Section 2.2. Furthermore, this search motivated us to research deeper on the pricing of assets that evolve under the Heston model, which will be presented in Section 2.5.

### 2.4.1 • The Cox-Ingersoll-Ross process

Here we use the same notation as in the paper "On the discretization schemes for the CIR (and Bessel squared) processes" [5]. We will assume that:

$$X_t = x_0 + \int_0^t (a - kX_s)ds + \sigma \int_0^t \sqrt{X_s} dW_s$$

With $x_0, \sigma, a \geq 0$, $k \in \mathbb{R}$. Furthermore, to guarantee that the process is always positive, we will ensure the following conditions:

$$2a > \sigma^2 \quad \text{and} \quad x_0 > 0$$

### 2.4.2 • Discretized schemes

Following the same notation as in the paper, we will denote $t_i = i\frac{T}{n}$, where $T$ is the total time of our simulation. We will denote a discrete scheme as $(\hat{X}^n_{t_i})_{i\in\{1,\dots,n\}}$. [5]

There are several ways to simulate the CIR process. Here we will develop two schemes that guarantee solutions that are positive and preserve the monotonicity property of CIR processes: if $x_0 < x_0'$ are two initial conditions, the scheme satisfies $\hat{X}^n_{t_i} < \hat{X}^{n'}_{t_i}$ [5]. We can use two different implicit methods in order to get the evolution of our process, the first by developing $X_t$ and taking an implicit scheme on the diffusion coefficient, and the second by applying Ito's Lemma to $X_t^{1/2}$ and taking an implicit scheme on the drift coefficient.

Let us start with the implicit scheme on the diffusion coefficient by developing $X_t$. Here we give the intuition behind the steps of the proof that is presented at [5], while also developing in more detail some parts of the proof. From the definition of $X_t$:

$$X_t = x_0 + \int_0^t (a - kX_s)ds + \sigma \int_0^t \sqrt{X_t} dW_s$$

We can therefore approximate $X_t$ as:

$$X_t \approx x_0 + \sum_{i=0}^{n} \mathbf{1}_{t_i<t}(a - kX_{t_{i+1}})\frac{T}{n} + \sigma \sum_{i=0}^{n} \mathbf{1}_{t_i<t}\sqrt{X_{t_i}}(W_{t_{i+1}} - W_{t_i})$$

$$\begin{aligned} X_t \approx x_0 &+ \sum_{i=0}^{n} \mathbf{1}_{t_i<t}(a - kX_{t_{i+1}})\frac{T}{n} \\ &+ \sigma \sum_{i=0}^{n} \mathbf{1}_{t_i<t}\sqrt{X_{t_i}}(W_{t_{i+1}} - W_{t_i}) \\ &+ \sigma \sum_{i=0}^{n} (\sqrt{X_{t_{i+1}}} - \sqrt{X_{t_{i+1}}})(W_{t_{i+1}} - W_{t_i}) \end{aligned}$$

$$\begin{aligned} X_t = x_0 &+ \sum_{i=0}^{n} (a - kX_{t_{i+1}})\frac{T}{n}. \\ &+ \sigma \sum_{i=0}^{n} \mathbf{1}_{t_i<t}\sqrt{X_{t_{i+1}}}(W_{t_{i+1}} - W_{t_i}) \\ &- \sigma \sum_{i=0}^{n} \mathbf{1}_{t_i<t}(\sqrt{X_{t_{i+1}}} - \sqrt{X_{t_i}})(W_{t_{i+1}} - W_{t_i}) \end{aligned}$$

Here we remark that $d\langle\sqrt{X}, W\rangle_s = \frac{\sigma}{2}ds$. This can easily be verified by applying Ito's lemma to $\sqrt{X}$:

$$d\sqrt{X_t} = \frac{1}{2\sqrt{X_t}}dX_t - \frac{1}{2}\frac{1}{4X_t^{\frac{3}{2}}}d\langle X_t\rangle_t$$

$$d\sqrt{X_t} = \frac{1}{2\sqrt{X_t}}((a - kX_t)dt + \sigma\sqrt{X_t}dW_t) - \frac{\sigma^2}{8\sqrt{X_t}}dt$$

$$d\sqrt{X_t} = \left(\frac{1}{2\sqrt{X_t}}(a - kX_t) - \frac{\sigma^2}{8\sqrt{X_t}}\right)dt + \frac{\sigma}{2}dW_t$$

$$d\sqrt{X_t} = \frac{a - \frac{\sigma^2}{4}}{2\sqrt{X_t}}dt - \frac{k}{2}\sqrt{X_t}dt + \frac{\sigma}{2}dW_t$$

Which proves that $d\langle\sqrt{X}, W\rangle_s = \frac{\sigma}{2}ds$. We can now replace

$$\sum_{i=0}^{n}\mathbf{1}_{t_i<t}(\sqrt{X_{t_{i+1}}} - \sqrt{X_{t_i}})(W_{t_{i+1}} - W_{t_i}) \approx \frac{\sigma}{2}\sum_{i=0}^{n}\mathbf{1}_{t_i<t}\frac{T}{n}$$

Hence:

$$X_t \approx x_0 + \sum_{i=0}^{n}\mathbf{1}_{t_i<t}\left(a - \frac{\sigma^2}{2} - kX_{t_{i+1}}\right)\frac{T}{n} + \sigma\sum_{i=0}^{n}\mathbf{1}_{t_i<t}\sqrt{X_{t_{i+1}}}(W_{t_{i+1}} - W_{t_i})$$

This leads to the following implicit scheme:

$$\hat{X}^n_{t_{i+1}} = \hat{X}^n_{t_i} + \left(a - \frac{\sigma^2}{2} - k\hat{X}^n_{t_{i+1}}\right)\frac{T}{n} + \sigma\sqrt{\hat{X}^n_{t_{i+1}}}(W_{t_{i+1}} - W_{t_i})$$

The unique positive root of our equation is then:

$$\hat{X}^n_{t_{i+1}} = \left(\frac{\sigma(W_{t_{i+1}} - W_{t_i}) + \sqrt{\sigma^2(W_{t_{i+1}} - W_{t_i})^2 + 4(\hat{X}^n_{t_i} + (a - \frac{\sigma^2}{2})\frac{T}{n})(1 + k\frac{T}{n})}}{2(1 + k\frac{T}{n})}\right)^2$$

Now let us develop the implicit method on the drift proposed by the paper. Recall from the previous proof that by applying Ito's lemma to $\sqrt{X_t}$ we obtain:

$$d\sqrt{X_t} = \frac{a - \frac{\sigma^2}{4}}{2\sqrt{X_t}}dt - \frac{k}{2}\sqrt{X_t}dt + \frac{\sigma}{2}dW_t$$

Hence:

$$\sqrt{X_t} \approx \sqrt{x_0} + \sum_{i=0}^{n}\mathbf{1}_{t_i<t}\left(\frac{a - \frac{\sigma^2}{4}}{2\sqrt{X_{t_{i+1}}}}\right)\frac{T}{n} - \sum_{i=0}^{n}\mathbf{1}_{t_i<t}\frac{k}{2}\sqrt{X_{t_{i+1}}}\frac{T}{n} + \frac{\sigma}{2}\sum_{i=0}^{n}\mathbf{1}_{t_i<t}(W_{t_{i+1}} - W_{t_i})$$

This leads to the following implicit scheme:

$$\sqrt{\hat{X}^n_{t_{i+1}}} = \sqrt{\hat{X}^n_{t_i}} + \left(\frac{a-\frac{\sigma^2}{4}}{2\sqrt{\hat{X}^n_{t_{i+1}}}}\right)\frac{T}{n} - \frac{k}{2}\sqrt{\hat{X}^n_{t_{i+1}}}\frac{T}{n} + \frac{\sigma}{2}(W_{t_{i+1}} - W_{t_i})$$

Multiplying both sides by $\sqrt{\hat{X}^n_{t_{i+1}}}$ we get:

$$\hat{X}^n_{t_{i+1}} = \sqrt{\hat{X}^n_{t_i}}\sqrt{\hat{X}^n_{t_{i+1}}} + \left(\frac{a-\frac{\sigma^2}{4}}{2}\right)\frac{T}{n} - \frac{k}{2}\hat{X}^n_{t_{i+1}}\frac{T}{n} + \frac{\sigma}{2}(W_{t_{i+1}} - W_{t_i})\sqrt{\hat{X}^n_{t_{i+1}}}$$

Which gives the same scheme as proposed in the paper [5] by rearranging the terms:

$$\left(1+\frac{kT}{2n}\right)\hat{X}^n_{t_{i+1}} - \left[\frac{\sigma}{2}(W_{t_{i+1}} - W_{t_i}) + \sqrt{\hat{X}^n_{t_i}}\right]\sqrt{\hat{X}^n_{t_{i+1}}} - \frac{a-\frac{\sigma^2}{4}}{2}\frac{T}{n} = 0$$

Having as solution:

$$\hat{X}^n_{t_{i+1}} = \left(\frac{\frac{\sigma}{2}(W_{t_{i+1}} - W_{t_i}) + \sqrt{\hat{X}^n_{t_i}} + \sqrt{(\frac{\sigma}{2}(W_{t_{i+1}} - W_{t_i}) + \sqrt{\hat{X}^n_{t_i}})^2 + 4\left(1+\frac{kT}{2n}\right)\frac{a-\frac{\sigma^2}{4}}{2}\frac{T}{n}}}{2\left(1+\frac{kT}{2n}\right)}\right)^2$$

Our simulations are based on the first method.

### 2.4.3 • Conclusion

In this section, we have explained the reasons why we have decided to shift our focus towards the discretization schemes of the Heston model. We have given the intuition behind the proofs presented in the paper [5] while also developing some details that were omitted. Now, with the robust scheme for the time evolution of the stochastic volatility of the Heston model, we are able to reproduce some of the results of the paper "A Tale of Two Time Scales." [2]

Interested in the model we studied in this section we shifted our attention towards the option price of assets that follow such dynamics. Since it is possible to obtain a closed form of the probability distribution of $S_t$, we got interested in the pricing of European call options using fast Fourier transforms (FFT), which will be detailed in the following section.

## 2.5 Option Valuation Using FFT

After studying how to build a discrete scheme for the Heston model, we got interested in the idea of learning more about the model itself. We shifted therefore our attention to the pricing of European options that have their dynamics as modeled by Heston. Interestingly, since it is possible to find the closed form of the characteristic function of the spot price of such assets, we can follow the steps proposed at "Option valuation using the fast Fourier transform" and apply Fast Fourier Transforms to perform that task [6]. In this section, we will develop the theory that is presented in the paper and apply that to the Heston model. Since under this setting, there are some numerical challenges due to the noncontinuity of the logarithm of a complex number, we will also present some of the concepts that we found at "Not-So-Complex Logarithms in the Heston Model" and used to be able to generate our results. [7]

### 2.5.1 • Pricing using characteristic functions

Here we will study the pricing of a European call of maturity $T$. We follow the same notation as presented in "Option valuation using the fast Fourier transform" [6]. The payoff of a European call option at maturity is written as:

$$\text{Payoff} = (S_T - K)^+$$

Where $S_T$ is the price at maturity of the given asset. In the following, we will keep the same notation as in the paper and approach the problem under the risk-neutral probability. Let us look at the risk-neutral density of the log price $s_T = \log(S_T)$ of density $q_T$. The characteristic function of the log price is therefore:

$$\phi_T(u) = \int_{-\infty}^{\infty} e^{ius} q_T(s) ds$$

Under the risk-neutral assumption, we have that the price $C_T(k)$ of a European call with strike log-strike $k$ ($k = \log(K)$) and maturity $T$:

$$C_T(k) = \int_k^{+\infty} e^{-rT}(e^s - e^k) q_T(s) ds$$

Since when $k \to -\infty$ we have that $C_T(k) \to S_0$, the price of the call is not square-integrable, and thus we perform the following adaptation:

$$c_T(k) := e^{\alpha k} C_T(k)$$

Which, for a certain range of values of $\alpha$ makes $c_T(k)$ a square integrable function in $k$. [6] Now let us perform the Fourier transform of $c_T(k)$:

$$\Psi(v) = \int_{-\infty}^{+\infty} e^{ivk} c_T(k) dk$$

Using the inverse Fourier transform, we can retrieve the call price:

$$C_T(k) = \frac{e^{-\alpha k}}{2\pi} \int_{-\infty}^{\infty} e^{-ivk} \Psi_T(v) dv$$

Since $C_T(k)$ is real:

$$C_T(k) = \frac{e^{-\alpha k}}{\pi} \int_{0}^{\infty} e^{-ivk} \Psi_T(v) dv$$

Now if we look back at the forward Fourier transform, may compute it explicitly:

$$\Psi_T(v) = \int_{-\infty}^{\infty} e^{ivk} \int_{k}^{+\infty} e^{\alpha k} e^{-rT} (e^s - e^k) q_T(s) ds dk$$

Inverting the integrals:

$$\Psi_T(v) = \int_{-\infty}^{\infty} e^{-rT} q_T(s) \int_{-\infty}^{s} (e^{s+\alpha k} - e^{1+\alpha k}) e^{ivk} dk ds$$

$$\Psi_T(v) = \int_{-\infty}^{\infty} e^{-rT} q_T(s) \left( \frac{e^{(\alpha+1+iv)s}}{\alpha + iv} - \frac{e^{(\alpha+1+iv)s}}{\alpha + 1 + iv} \right) ds$$

$$\Psi_T(v) = \frac{e^{-rT}}{\alpha^2 + \alpha - v^2 + i(2\alpha+1)v} \int_{-\infty}^{\infty} e^{i(v-(\alpha+1)i)s} q_T(s) ds$$

Which is exactly, by using the characteristic function of the log price:

$$\Psi_T(v) = \frac{e^{-rT} \phi_T(v - (\alpha+1)i)}{\alpha^2 + \alpha - v^2 + i(2\alpha+1)v}$$

Hence, we could replace that on our equation for $C_T(k)$:

$$C_T(k) = \frac{e^{-\alpha k}}{\pi} \int_{0}^{\infty} e^{-ivk} \Psi_T(v) dv$$

To obtain the price of our call. We remark that this is simply a direct Fourier transform. As indicated in the paper, we remark that the denominator vanishes when both $\alpha = 0$ and $v = 0$, inducing a singularity, which reinforces the choice of adding $\alpha \neq 0$ for integrability purposes.

### 2.5.2 • On the FFT

Now we move to the numerical part of the problem. Here we attempt to rewrite the integration of the previous section as a summation that allows direct application of the FFT.
Set $v_j = \eta(j-1)$. Using the trapezoid rule on the integral:

$$C_T(k) \approx \frac{e^{-\alpha k}}{\pi} \sum_{j=1}^{N} e^{-iv_j k} \Psi_T(v_j) \eta$$

Which we do by setting the upper limit of our integral at $a = N\eta$. In other words, we simply fixed $a$ to be the limit of our integral and created a grid with $N$ steps in our summation. Since we are interested in at-the-money call values we are looking at values of $k$ that are near $S_T$.

The FFT shall return $N$ values of $k$ to which we employ a regular spacing of size $\lambda$, hence, our values of $k$ are:

$$k_u = -b + \lambda(u-1), \quad u \in \{1, \dots, N\}$$

now replace substitute these values on our summation:

$$C_T(k_u) \approx \frac{e^{-\alpha k_u}}{\pi} \sum_{j=1}^{N} e^{-iv_j k_u} \Psi_T(v_j)\eta$$

$$C_T(k_u) \approx \frac{e^{-\alpha k_u}}{\pi} \sum_{j=1}^{N} e^{-iv_j[-b+\lambda(u-1)]} \Psi_T(v_j)\eta$$

$$C_T(k_u) \approx \frac{e^{-\alpha k_u}}{\pi} \sum_{j=1}^{N} e^{-iv_j\lambda(u-1)} e^{ibv_j} \Psi_T(v_j)\eta$$

We can also replace $v_j$:

$$C_T(k_u) \approx \frac{e^{-\alpha k_u}}{\pi} \sum_{j=1}^{N} e^{-i\eta\lambda(j-1)(u-1)} e^{ibv_j} \Psi_T(v_j)\eta$$

To apply the fast Fourier transform we must guarantee, therefore:

$$\lambda\eta = \frac{2\pi}{N}$$

Hence there is a clear trade-off between having a fine grid with $\eta$ small and having a small space between the values of $k_u$ that we can compute. To be able to maintain accurate enough integration with larger values of $\eta$ we can incorporate Simpson's rule (composite Simpson's 1/3 rule), rewriting our summation as:

$$C_T(k_u) \approx \frac{e^{-\alpha k_u}}{\pi} \sum_{j=1}^{N} e^{-i\frac{2\pi}{N}(j-1)(u-1)} e^{ibv_j} \Psi_T(v_j) \frac{\eta}{3}[3 + (-1)^j - \delta_{j-1}]$$

It is our task to therefore choose appropriately $a$, $N$, and $\alpha$.

### 2.5.3 • Obtaining Heston's characteristic function

Before moving towards our simulation, we will develop on how to obtain the characteristic function of the log-price distribution of an asset price at maturity under the Heston model. We recall that the Heston stochastic model is given by the system of SDE :

$$dS_t = \mu S_t dt + \sqrt{V_t} S_t dW_S(t)$$

$$dV_t = \kappa(\theta - V_t)dt + \omega\sqrt{V_t} dW_V(t)$$

with correlated Brownian motions $dW_S(t)dW_V(t) = \rho dt$, and two initial state $S_0$ and $V_0$.

We recall the characteristic function of $S_t$ :

$$\phi(u) = \mathbb{E}[S_t^{iu}] = \mathbb{E}[e^{iu\ln(S_T)}]$$

You can find the computation of the characteristic function in the original paper of Heston, and it's defined as follows:

$$\phi(u) = e^{C(u)+D(u)V_0+iu\ln F}$$

Where

$$F = S_0 e^{\mu T}$$

$$C(u) = \frac{\kappa\theta}{\omega^2}\left((\kappa - \rho\omega ui + d(u))T - 2\ln\left(\frac{c(u)e^{d(u)T}-1}{c(u)-1}\right)\right)$$

$$D(u) = \frac{\kappa - \rho\omega ui + d(u)}{\omega^2}\cdot\frac{e^{d(u)T}-1}{c(u)e^{d(u)T}-1}$$

with

$$c(u) = \frac{\kappa - \rho\omega ui + d(u)}{\kappa - \rho\omega ui - d(u)}, \qquad d(u) = \sqrt{(\rho\omega ui - \kappa)^2 + iu\omega^2 + \omega^2 u^2}$$

One can notice that these equations make use of the logarithm of complex numbers, which is a function that could have multiplied definition, and not continuous.
for example, if $z = x + iy = r_z e^{it_z}$ where $t_z \in ]-\pi, \pi]$, the logarithm of $z$ in python libraries is :

$$\log(z) = \log(r_z) + it_z$$

Called the principal branch.

We studied the paper of C.Kahl, and P.Jackel [7], where the authors pointed out the errors of option pricing involving the Heston stochastic model due to the evaluation of a complex argument. The paper proposes an alternative to solve this issue, that guarantees the continuity of the $\phi(u)$
First of all, we write in another way the characteristic function :

$$\phi(u) = G(u)^{-2\gamma} e^{R(u)+D(u)V_0+iu\ln F}$$

where

$$G(u) = \frac{c(u)e^{d(u)T}-1}{c(u)-1}, \quad R(u) = \gamma(\kappa - \rho\omega ui + d(u))T, \quad \gamma = \frac{\kappa\theta}{\omega^2}$$

As such $C(u) = R(u) - 2\gamma\ln G(u)$
Now we reduce the problem on the computation of $\ln G(u)$, to do the computation, the paper introduces the following quantities :

$$c = r_c e^{it_c}$$

$$d = a_d + ib_d$$
$$c - 1 = r^* e^{i(\chi^* + 2\pi m)}$$

where $m = [(t_c + \phi)/(2\pi)]$, $\chi^* = arg(c-1)$ and $r^* = |c-1|$

$$ce^{dT} - 1 = r^{**} e^{i(\chi^{**} + 2\pi n)}$$

where $n = [(t_c + b_d T + \pi)/(2\pi)]$, $\chi^* = arg(ce^{dT} - 1)$ and $r^* = |ce^{dT} - 1|$

with these defined variables we obtain :

$$G(u) = \frac{ce^{dT} - 1}{c - 1} = \frac{r^*}{r^{**}} e^{\chi^{**} - \chi^* + 2\pi(n-m)}$$

Hence the logarithm of $G(u)$ can be expressed as :

$$\ln G(u) = \ln(\frac{r^*}{r^{**}}) + i[\chi^{**} - \chi^* + 2\pi(n-m)]$$

**Remark.** *With this definition of the logarithm, the corresponding argument of $G(u)$ is :*

$$arg(G(u)) = \chi^{**} - \chi^* + 2\pi(n-m)$$

*The following figure is a comparison between this new definition of the argument of $G(u)$ and the principal branch (the common definition of the argument of a complex number in $(-\pi, \pi]$).*

*We can observe the discontinuity in the case of the default function of $arg$, and its correction.*

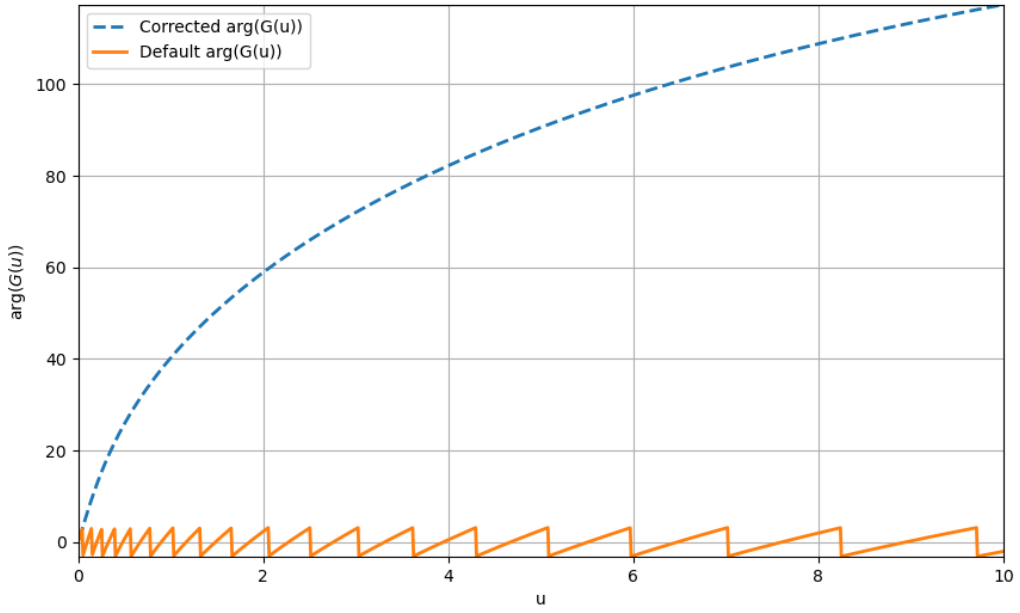


Figure 11: The phase of $G(u)$ with the new definition (dashed) and with the default one (solid) for $\kappa = 1$, $T = 30$, $\rho = -0.95$ and $\omega = 1.4$

### 2.5.4 • Pricing options

Now that we have the characteristic function and the expression of fast Fourier transformation of the European Call Price, we can start a simulation to predict the call price for different K.

**Remark.** *In [6], on the choice of $\alpha$, the authors showed that $\alpha$ need to verify $\mathbb{E}[S_T^{1+\alpha}] < \infty$ We tried different values of $\alpha$ in our simulation, and the figure below shows the difference.*


Figure 12: The Price of the European Call as a function of the strike $K$, with different value of $\alpha$

To verify that our results are accurate, we choose to perform a Monte Carlo Simulation. The parameters are :

$$
\begin{aligned}
S_0 &= 1, && \text{(Initial stock price)} \\
V_0 &= 0.2, && \text{(Initial volatility)} \\
T &= 1, && \text{(Time to maturity)} \\
\mu &= 0, && \text{(Expected return)} \\
r &= \mu, && \text{(Risk-free interest rate)} \\
\kappa &= 1, && \text{(Rate of reversion)} \\
\theta &= 0.4, && \text{(Long-run average volatility)} \\
\omega &= 0.3, && \text{(Volatility of volatility)} \\
\rho &= -0.2 && \text{(Correlation between stock and volatility)}
\end{aligned}
$$

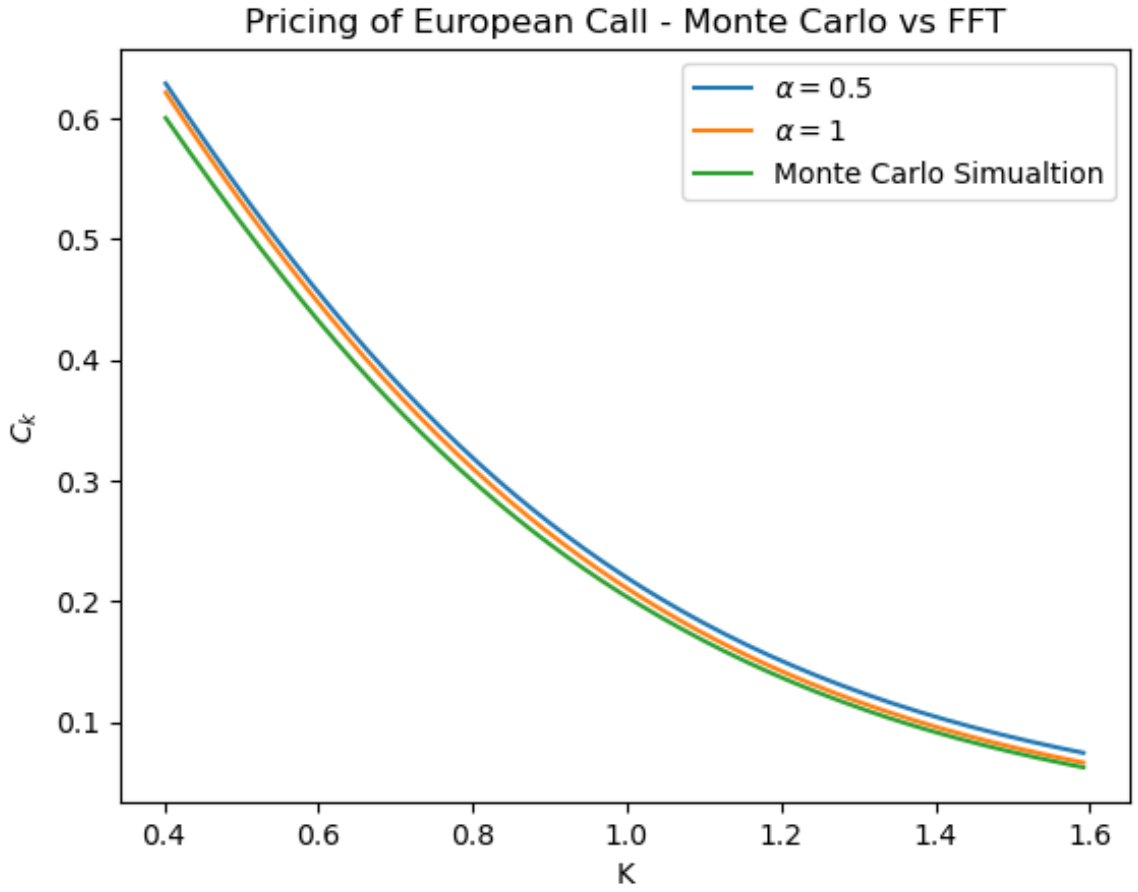


### 2.5.5 • Conclusion

Based on the plot provided, which compares the pricing of European call options using the Fast Fourier Transform (FFT) method against Monte Carlo simulations for different values of $\alpha$, we can conclude that the FFT method shows a high degree of accuracy. The overlapping lines in the plot indicate that the pricing obtained through the FFT method aligns closely with the results from the Monte Carlo simulations.

The consistency across different values of $\alpha$ suggests that the FFT method is robust and performs well across a range of scenarios. Given the computational efficiency of FFT compared to the potentially time-consuming Monte Carlo simulations, especially for a large number of simulations or complex option pricing models, the FFT method emerges as a valuable tool for practitioners in the field of financial analysis and option pricing.

# 3 CONCLUSION

The course MAP511 - Initiation to Research was a unique opportunity to have first contact with the research that is being done in Applied Mathematics on the subject of Financial modeling and engineering - High-frequency statistics and market microstructure. Over the course of these past months, we were able to explore the challenge of volatility estimation when the time span of trades is heavily influenced by market microstructure, learning from excellent papers that shaped the research in this field. Furthermore, we also explored the challenges of simulating the Heston model scheme, learning in the process robust methods to simulate it, a key step that allowed us to improve the results we obtained in Section 2.2. Moreover, following an interest in the Heston model, we delved into the study of option pricing using a fast Fourier transform.

Here we summarize the main learning aspects or findings of each section of this report:

- Optimal Execution (Section 2.1): Study on how to model the risk-averseness of a trader by a utility function and how to obtain the optimal portfolio liquidation strategy under permanent and temporary market impact of trader actions. Moreover, we were able to compute the *efficient frontier* that corresponds to the expected loss of a trader given its risk-averseness, as well as the impact on their utility function given the miscalculation of asset volatility.

- Integrated Volatility (Section 2.2): Study on how to estimate asset volatility when the asset price is impacted by market microstructure. We were able to reproduce the main curves and results of the paper and got the intuition of why market microstructure can impact volatility prediction.

- Uncertainty Zones (Section 2.3): Study on how to more accurately take into account market microstructure impact of the price of assets. We learned how to simulate such markets, as well as how to implement estimators that are robust with the discretization of prices due to tick size. We were able to visualize the limitations of the previous methods that we explored, highlighting the improvements in the volatility estimation learned in this section.

- CIR Schemes for Heston Model (Section 2.4): Study on how to properly generate the price of assets under Heston schemes. This step was crucial for developing robust simulations for the studies of the other sections. We went into more detail on some of the proofs of the supporting paper of this section and demonstrated the steps to arrive at the discretization formula provided by the paper under the implicit scheme on the diffusion and drift coefficients.

- Option Valuation Using FFT (Section 2.5): Study of the pricing of European calls for assets that follow the Heston model. We develop the analytical equations that demonstrate the usage of FFT for option pricing. We also implement the FFT, approaching the

problem of the continuity of the logarithm of a complex number. In the end, we present a comparison with a simple Monte Carlo simulation for option pricing, confirming our results and the advantage of FFT given its faster execution.

In conclusion, the research we conducted over the past months was a very enriching experience. It allowed us to not only have first contact with academic research in the field of Financial modeling and engineering but also deepen the knowledge we acquired in courses that we took this semester, such as MAP552 - Stochastic Calculus in Finance. When attempting to reproduce the results obtained in the papers, we believe we acquired a better understanding of the main concepts of the papers. It gave a stable foundation from which we could draw intersections between them and explore new ideas. This approach, along with all the skills and background in the literature that we acquired, will definitely be key factors in our future research endeavors.

# REFERENCES


[1] Robert Almgren and Neil Chriss (2000). Optimal Execution of Portfolio Transactions, Journal of Risk, DOI: 10.21314/JOR.2001.041

[2] Lan Zhang, Per A Mykland & Yacine Aït-Sahalia (2005). A Tale of Two Time Scales, Journal of the American Statistical Association, 100:472, 1394-1411, DOI: 10.1198/016214505000000169

[3] Christian Y. Robert, Mathieu Rosenbaum (2011). A New Approach for the Dynamics of Ultra-High-Frequency Data: The Model with Uncertainty Zones, Journal of Financial Econometrics, Volume 9, Issue 2, Spring 2011, Pages 344–366, https://doi.org/10.1093/jjfinec/nbq023

[4] Robert, C. Y. and M. Rosenbaum (2011). Volatility and covariation estimation when microstructure noise and trading times are endogenous. Journal of Financial Econometrics 9 (2), 344–366. https://onlinelibrary.wiley.com/doi/10.1111/j.1467-9965.2010.00454.x

[5] Alfonsi, A. (2005). On the discretization schemes for the CIR (and Bessel squared) processes. Monte Carlo Methods and Applications, 11(4), 355-384. DOI: 10.1515/156939605777438569

[6] Peter Carr and Dilip B. Madan (2000). Option valuation using the fast Fourier transform, Journal of Computational Finance, DOI: 10.21314/JCF.1999.043

[7] Kahl, C. and Jackel, P. (2005) Not-So-Complex Logarithms in the Heston Model. Wilmott Magazine, 19, 94-103. DOI: https://wilmott.com/not-so-complex-logarithms-in-the-heston-model/

[8] Heston, S. (1993): A closed-form solution for options with stochastic volatility with applications to bond and currency options, Review of Financial Studies 6, 327-343. https://www.jstor.org/stable/2962057